Quantum interference in attosecond transient absorption of laser-dressed helium atoms

Shaohao Chen, Mengxi Wu, Mette B. Gaarde, and Kenneth J. Schafer

Phys. Rev. A **87**, 033408 — Published 8 March 2013

DOI: 10.1103/PhysRevA.87.033408

Quantum interference in attosecond transient absorption of laser-dressed helium atoms

Shaohao Chen, Mengxi Wu, Mette B. Gaarde, and Kenneth J. Schafer
Department of Physics and Astronomy, Louisiana State University, Baton Rouge 70803, USA
(Dated: February 22, 2013)

We calculate the transient absorption of an isolated attosecond pulse (IAP) by helium atoms subject to a delayed infrared (IR) laser pulse. With the central frequency of the broad attosecond spectrum near the ionization threshold, the absorption spectrum is strongly modulated at the sub-IR-cycle level. Given that the absorption spectrum results from a time-integrated measurement, we investigate the extent to which the delay-dependence of the absorption yields information about the attosecond dynamics of the atom-field energy exchange. We find two configurations in which this is possible. The first involves multi photon transitions between bound states that result in interference between different excitation pathways. The second involves the modification of the bound state absorption lines by the IR field, which we find can result in a sub-cycle time dependence only when ionization limits the duration of the strong field interaction.

PACS numbers: 32.80.Qk,32.80.Rm

Attosecond transient absorption (ATA) studies provide a way to push our understanding of the energy transfer between electromagnetic fields and matter to the subfemtosecond time scale [1, 2]. They are an all-optical attosecond metrology that complements methods based on the measurement of charged particles, such as attosecond streaking [3, 4] and electron interferometry [5, 6]. Like those methods, high time-resolution is gained in an ATA spectrometer by using attosecond extreme ultraviolet (XUV) pulses that are synchronized to the field oscillations of an infrared (IR) laser pulse. The first ATA experiments used an attosecond pulse to probe a valence electron wave packet (EWP) created by ionizing an atom with a strong IR laser pulse [1, 7]. Recent ATA experiments have used attosecond pulses as a *pump* that creates an EWP which is then probed by a moderately strong IR field. In this XUV-pump/IR-probe configuration the frequency-resolved transient absorption signal varies as a function of the IR intensity, duration, and the sub-cycle timing between the two fields [8–10]. These experiments raise the possibility of studying time-dependent absorption down to the attosecond time scale.

In this theoretical study, similar to recent experiments [10, 11], we consider helium atoms that are excited by an isolated attosecond pulse (IAP) with a central frequency near the ionization threshold, together with a delayed few-cycle IR pulse. We elucidate the key features of the resulting delay-dependent attosecond absorption (DDAA) spectra. These features derive from the fact that the IAP "starts the clock" by exciting the system at a well-defined time, and that it makes an EWP that is essentially independent of the pump-probe delay. The DDAA measurement is a spectrogram that records the interference between different excitation pathways which lead to the same absorption or emission processes. Because the attosecond pulse is locked to the IR field oscillations, it is suggestive that many of the features in the spectrum are modulated at half the IR laser period ($T_{\rm IR}$), about 1.3 fs. However, the absorption spectrum results from the time-integrated response of everything that happens after the initial XUV excitation, which complicates the analysis. Our main concern in this paper is the connection between these oscillations and the real-time attosecond dynamics.

We discuss two distinct manifestations of attosecond dynamics in the DDAA spectrum. First, near the ionization threshold the delay-dependent absorption exhibits fully modulated interference fringes at half the IR period. We show these are due to the interference between two pathways, separated in time, which give rise to the same dipole response. This "which way" quantum path interference [12] can be used to time-resolve two photon transitions between excited states, and shows how the absorption at XUV frequencies is altered on a sub-cycle time scale. We find $T_{\rm IR}/2$ oscillations with a similar origin in absorption features associated with nonlinear XUV+IR processes, which appear as light-induced structures in the ATA spectrum. These fringes illustrate how energy can be exchanged between excitation modes (dressed states) that exist only when the XUV and IR fields overlap in time. The second feature results from the IR driven sub-cycle AC Stark shift of the lower-lying $2p$ and $3p$ resonances [10]. The time-dependent Stark shift leads to a dispersive line-shape, which results from interference between the time-dependent dipole induced before, during, and after the IR pulse. We show that, due to the integrated nature of the absorption spectrum, a measurement of the instantaneous energy shift is only possible when ionization limits the interaction time.

The essential features of DDAA spectra can be understood at the single atom level. The energy lost or gained by a light field in the interaction with an atom can be described by a frequency-dependent response function $\tilde{S}(\omega, t_d) = 2\,\mathrm{Im}[\tilde{d}(\omega, t_d)\tilde{\mathcal{E}}^*(\omega, t_d)]$, where t_d is the pump-probe delay (we use atomic units unless otherwise indicated). $\tilde{d}(\omega, t_d)$ and $\tilde{\mathcal{E}}(\omega, t_d)$ are the Fourier transforms of the time-dependent dipole moment $d(t)$ and the total driving field $E(t)$ for a given pump-probe delay. The dipole moment is obtained by solving the time-dependent

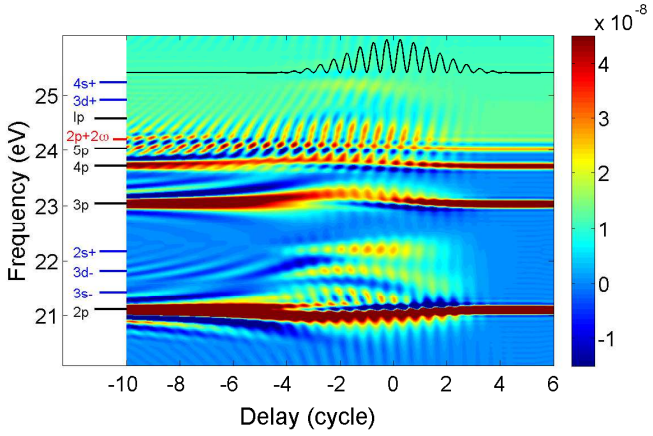

FIG. 1: Single atom response function $\tilde{S}(\omega, t_d)$ in helium where t_d is the time delay in IR cycles between the IR laser pulse (800 nm, 3×10^{12} W/cm^2, 4 cycles, cos^2 envelope, sine-like carrier envelope) and the attosecond pulse (330 as, centered at 25 eV). The IR intensity oscillations are shown in black in the top panel.

Schrödinger equation (TDSE) in the single-active-electron approximation [13]. We include a dipole dephasing time T_2 in the calculations by smoothly windowing the dipole moment over a time which is much longer than the length of the IR pulse we study. This simulates the effect of, for example, collisional broadening and finite detector resolution, which are present in experiments but absent from TDSE calculations.

Fig. 1 shows a typical response function vs pump-probe delay. The 25 eV, 330 as IAP pump pulse has a bandwidth of 5.5 eV, which means that it overlaps all the singly excited and low-energy continuum states of the He atom. The FWHM of the 800 nm probe pulse is 11 fs, corresponding to 4 optical cycles ($T_{\rm IR} = 2.7$ fs). The IR field is of moderate intensity, so that it can not itself excite the atom in its ground state. The pump and probe fields have parallel linear polarizations. We use a dipole dephasing time $T_2 = 65$ fs. The value chosen yields a minimum line width ($\sim .08$ eV) which is in line with the spectral resolution for current ATA experiments [10, 11]. We have verified that using a longer T_2 does not change any of our conclusions, which is expected since 65 fs is already much longer than the IR pulse length we study. Note that positive or negative values of $\tilde{S}(\omega, t_d)$ mean that a dilute gas will absorb or emit energy at frequency ω as the dipole-driven source term in the wave equation will be either out phase or in phase with $\tilde{\mathcal{E}}(\omega)$ [13, 14].

We begin by briefly describing the main features in Fig. 1. For large positive delays, $t_d \geq 4\,T_{\rm IR}$, the IAP arrives after the end of IR pulse and the absorption spectrum exhibits only one-XUV-photon transitions from the ground state to the np states. When the two pulses overlap, $-4\,T_{\rm IR} < t_d < 4\,T_{\rm IR}$, these absorption features are strongly modified. In this same delay range, light-induced structures (LISs) appear, for example, between the $2p$ and $3p$ resonant lines. These are associated with two-photon (XUV$\pm$IR) processes that transfer population from the ground state to non-dipole coupled ("dark") s and d states, and have recently been observed experimentally [11]. Finally, when the IAP arrives before the IR pulse, $t_d \leq -4\,T_{\rm IR}$, the dipole established by the XUV pulse undergoes free decay until the IR pulse arrives and strongly modified the dipole, which induces sidebands on the main resonance features [15, 16].

Many of the features in $\tilde{S}(\omega, t_d)$ show a modulation at one half the laser period. Of particular interest are fringes that are present both when the pulses overlap and when the IAP arrives before the IR. An example is seen in Fig. 1 between 24.2 and 24.8 eV near the label "$2p + 2\omega$", also shown in more detail in Fig. 2(b). These fringes are caused by quantum interference between two distinct pathways for establishing the same coherence between the ground state and a group of np states (n > 5), near threshold. The process is diagrammed in Fig. 2(a). The direct pathway is an XUV-driven 1st-order process that populates all of the np states simultaneously in a manner that is independent of the delay. The indirect pathway is a 3rd-order process in which amplitude in the $2p$ states is transferred to an np state by a two-IR-photon process. The role of the indirect pathway via the $2p$ state is confirmed by a test calculation which dynamically eliminates the $2p$ state during the time-propagation of the TDSE, in which these fringes disappear. The two interfering processes, since they are driven by the XUV field and the IR field respectively, happen at different times depending on the value of t_d. The resulting interference fringes are analogous to those observed in photoelectron spectra [6], however, in DDAA the multiphoton process need not result in ionization.

Having identified the interfering pathways it is then straightforward to write down the condition for constructive interference as a function of delay:

$$(\omega_{np} - \omega_{2p})|t_d - t_0| + \Delta\phi = 2\pi k, \qquad (1)$$

where ω_{np} and ω_{2p} are the energies of the np and $2p$ states respectively and k is a positive integer [6]. We expect this condition to apply when the XUV precedes the peak of the IR pulse, $t_d < 0$. It correctly predicts a decreasing slope for the fringes as $|t_d - t_0|$ increases, corresponding to increasing k in Eq. (1). To use the constructive interference condition quantitatively, two additional parameters enter: $\Delta\phi$ is a phase due to the two-IR-photon transition, and t_0 is the time when the two photon transition probability peaks. We can then fit the interference fringes for $t_d < 0$ using one set of integers k that start with $k = 1$ at t_0 and varying $\Delta\phi$ to obtain the best overall agreement with the calculation. The result for 800 nm IR pulse is shown in Fig. 2(b). We obtain an excellent fit with $t_0 = -T_{\rm IR}/4$ and $\Delta\phi = 0$. The value of t_0 corresponds to the peak of the IR field due to the sine-like IR carrier wave used in the calculation. For $t_d > 0$ the biggest contribution to the indirect pathway comes from whatever IR field maximum follows the XUV pulse (never more than one half cycle away). The slope of the fringes should

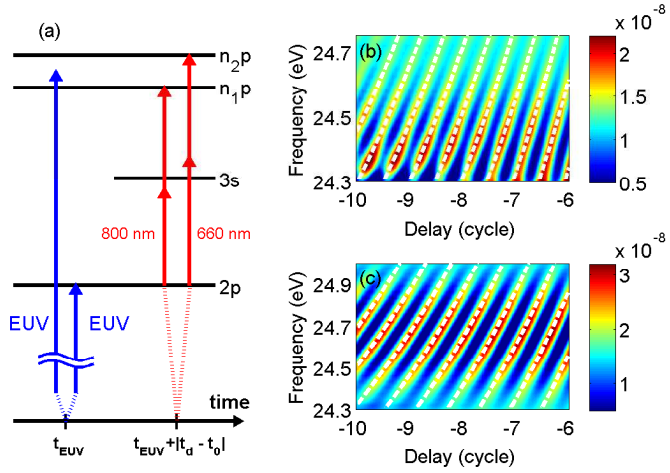

FIG. 2: (a) Diagram of direct (one-photon) and indirect (three-photon) pathways to the same final n_1p (or n_2p) states. Comparison of absorption maxima and the constructive interference condition (white dashed curves) for a narrow range of frequencies and IR wavelengths of (b) 800 nm (same as Fig. 1) and (c) 660 nm.

therefore saturate for $t_d > 0$, which is indeed what we observe in Fig. 1. We can thus conclude that the strength of the two photon transition peaks at the local intensity maxima of the IR field. This supports a time-dependent picture of multi-photon absorption below threshold as a process that follows the sub-cycle oscillations of the IR electric field.

One application of this 1st vs. 3rd order interference process is illustrated in Fig. 2(a). Realizing that the indirect pathway is enhanced due to a near one-IR-photon resonance with the intermediate $3s$ state, it seems possible that we can use this to study the variation in the phase $\Delta\phi$ in Eq. (1) as we scan the IR frequency near an intermediate resonance. For an 800 nm pulse we found that $\Delta\phi = 0$, as could be expected from second order perturbation theory, because the intermediate $3s$ state lies above the energy reached by absorbing one IR photon from the $2p$ state [17]. In Fig. 2(c) we have repeated the calculation in Fig. 1 using a wavelength of 660 nm. Since the absorption of one photon now reaches an energy safely above the $3s$ state, the sign of all the two photon matrix elements is flipped, and we expect this phase should shift by π. In Fig. 2(c) we find that indeed the best fit is given by $\Delta\phi = \pi$. The interference fringes can therefore be used to measure the phase of an intermediate resonance if the pulse wavelength can be scanned. An experimental study of the phase of an intermediate resonance, similar to what we propose here, was carried out using the detection of above threshold photoelectrons in [18]. Another, more speculative application, is as a probe of decoherence. A short decoherence time would reduce the fringe contrast for large negative delays, from which the time scale for decoherence could be inferred directly.

We can apply a similar analysis based on interfering two photon processes to the fringes in the LISs as well. These appear only in the overlap region ($-4\,T_{\rm IR} < t_d < 4\,T_{\rm IR}$) and each LIS is associated with an s or d bound state which is coupled to the ground state by one XUV photon and the absorption or emission of an additional IR photon. We use a plus or minus label for LIS that are one photon above or below the final s or d state. LISs associated with coupling of the ground state to the $3s$, $3d$, and $2s$ states can be seen near 21.3 eV ($3s_-$), 21.7 eV ($3d_-$), and 22.1 eV ($2s_+$), respectively. Similar LISs are visible above threshold ($3s_+$, $3d_+$ and $4s_+$), where they are laser-induced continuum structures (LICS) [19]. The half cycle modulations in the LISs come from the $2\omega_{\rm IR}$ coupling of plus and minus LISs, which have an atomic state as an intermediate resonance. For example, the $3d_-$ is two-photon resonantly coupled to the $3d_+$ (visible near 25 eV around $t_d = -1\,T_{IR}$), yielding oscillations that are exactly out of phase with each other. These couplings can also be confirmed by examining the tilt of the LIS interference fringes. Eq. (1) predicts that the fringes of the $3d_-$ have a negative slope with respect to delay, which is indeed the case in Fig. 1. However, the fringes in $2s_+$ LIS have a positive slope, characteristic of being above the final $2s$ state. Fits to Eq. (1) using the LIS energies show that the two photon transitions between LISs also follow the maxima of the IR electric field oscillation.

Fig. 3 further demonstrates the generic nature of the half IR-cycle oscillations seen in the absorption spectra by showing them to be insensitive to the peak IR intensity. We show the total $2s_+$ and $3d_-$ absorption probabilities, calculated as the integral of the response function around the energy of each feature, for two different IR intensities. Though the yield at the LIS features increases with intensity, the fringe contrast of both absorption features are remarkably unchanged.This is because the position of the fringes is determined by the interference between a direct excitation and an indirect excitation such as in Eq. (1), with an intermediate state which is always one-IR-photon resonant by construction. Fig. 3 shows that the IR field does not add an additional intensity-dependent phase in this case.

A time-dependent perspective on the oscillations in the LISs that appear when the pump and probe overlap is provided by the observation that the coupling between the one-XUV-photon resonant np state and nearby dark states is in a regime where the rotating wave approximation breaks down, and that the short duration of the IAP yields a well-defined phase of the IR field at excitation. In such situations it has been demonstrated that the final state populations are sensitive to the phase of the laser at the time of excitation [20]. Here we have shown that the DDAA spectrum shows the same sensitivity.

We turn now to another possible source of fast dynamics in the transient absorption spectrum, which is the sub-cycle AC Stark shift of the bound state energies [10]. Figs. 3(a) and (b) show the evolution of the $2p$ and $3p$ line shapes with delay, which include both emission

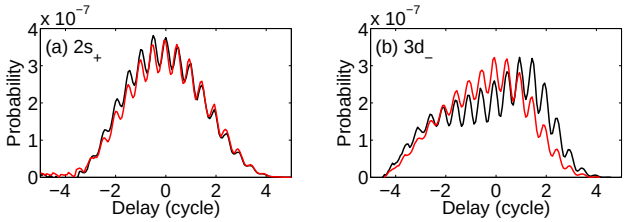

FIG. 3: Caption: (Color online) The delay-dependent absorption probability around the (a) 2s+ and (b) 3d- features, for intensities of 3e12 W/cm2 and 1e12 W/cm2 (shown in black and red, respectively). The lower intensity (red) curves have been scaled by a factor of 3 in (a) and 1.3 in (b) for better comparison.

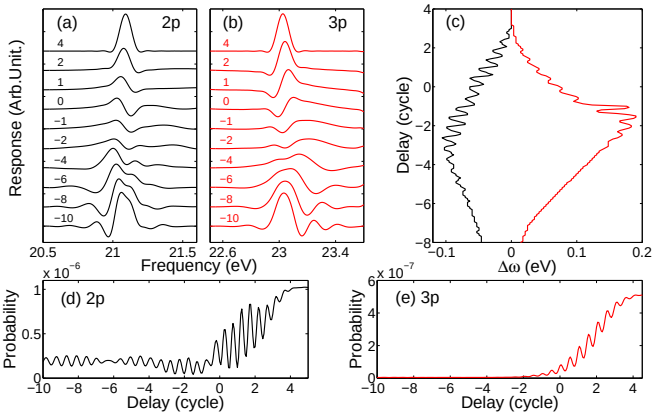

FIG. 4: Response as a function of frequency at around 2p (a) and 3p (b) resonance (lineouts of Fig. 1 at different delays). Energy shifts retrieved from the maximum response (c) for 2p (black) and 3p (red) states. Half-cycle modulation of absorption strength shown in integration of response function (black and red), as well as in final populations at the end of the pulses for 2p (d) and 3p (e) states.

and absorption. Qualitatively, this results from the redistribution of XUV energy across the resonances due to the perturbation of the dipole by the IR field. Similar dispersive line shapes have been discussed previously in connection with the control of exciton polarizations of a quantum dot using picosecond laser pulses [21, 22].

In a time-domain picture, the dispersive shape of the np absorption lines is caused by multiple contributions to the dipole moment: (i) a perturbed response during the IR pulse, and (ii) free decay of the coherence after the IR pulse ends [15, 23]. The relative importance of these terms is determined by the IR field intensity and delay, as well as the dephasing time T_2. If the state amplitude is unchanged by the IR field then the main contribution to the dipole moment comes from the free decay which, however, acquires a phase shift, θ_S, equal to the integrated optical Stark shift during the time when the IR pulse acts [7, 15, 23, 24]. In this approximation the response is given by

$$\tilde{S}(\omega, t_d) \approx \mathcal{L}(\omega, T_2)\,[\cos(\theta_S) + (\Delta \cdot T_2)\sin(\theta_S)] \qquad (2)$$

where Δ is the difference $\omega - \omega_{np}$ and $\mathcal{L}(\omega, T_2)$ is the line shape in the absence of the IR field, a Lorentzian or the one electron excitation considered here. For positive delays $1 \leq t_d < 4T_{IR}$ we find that the line shape is well described by this simple form. We see that the shift of the absorption is in the *direction* of the Stark shift, but the magnitude of the shift is proportional to θ_S/T_2 and is therefore constrained by the linewidth. Thus, for these delays, the 2p and 3p lines have Stark shifts of opposite sign, as shown in Fig. 3(c), but the magnitude of these shifts does not generally equal the instantaneous Stark shift and so does not carry attosecond information.

At delays near zero ($-4\,T_{IR} \leq t_d < 1\,T_{IR}$) the lineshape becomes much wider than $1/T_2$ and more complex than the simple dispersive shape discussed above. Here depopulation of the excited states by the IR field plays a larger role (see the final state populations plotted in Fig. 3(d-e)), and the response is dominated by the perturbed dipole decay. For the 3p state the loss is predominantly by one photon ionization to the continuum and the dipole response exists for only a few laser cycles after it is excited. This rapid ionization-induced dephasing allows us to probe the real-time sub-cycle dynamics using a delay-dependent method: during this time (near -2 T_{IR} in Fig. 3(c)) we observe a large transient shift of the 3p feature of about 0.19 eV, comparable to the ponderomotive energy of 0.18 eV, and strong half cycle oscillations in the peak position, showing the rapid variation in the energy of the resonance as it follows the IR field oscillations. These observations are in line with other investigations which show that the Stark shift is difficult to observe optically in the absence of rapid dephasing [7]. This means that observing fast dynamics via ionization-induced dephasing requires careful control of the IR intensity. Above threshold, however, any dipole oscillation rapidly dies out as the overlap between the continuum wave packet and the ground state goes to zero in a short time, hence the effective dephasing is very rapid. This means that above threshold we always observe an overall ponderomotive shift of the absorption, but the response is very weak.

The behavior of the peak of the 2p lineshape is more complex than the 3p, in part because the 2p is never fully depopulated during the IR pulse (Fig. 3 (d)), and in part because of the strong coherent coupling between the 2p state and the nearby dark states. The 2p lineshape therefore always results from both perturbed and free decay. The sub-cycle oscillations of the 2p position are most likely due to the which-way interference with the np states discussed in the context of Fig. 2, judging from the negative and changing slope of the fringes between $-3\,T_{IR}$ and $3\,T_{IR}$ (as seen in Fig. 1). As such they do *not* contain information about the sub-cycle AC Stark shift.

For delays $t_d < -4T_{IR}$ the IAP and IR act separately: the dipole established by the IAP oscillates freely until the IR pulse strongly perturbs it, greatly altering the dipole amplitude and phase in a few IR cycles. This perturbed free polarization decay has been observed previ-

ously at optical frequencies [15, 16]. It yields sidebands, seen clearly above the $3p$ and below the $2p$ lines, with a characteristic hyperbolic shape that depends on the delay as $1/t_d$ and shows no attosecond time scale dynamics.

To conclude, we have identified two configurations where attosecond dynamics can be observed in attosecond transient absorption spectra: which-way interference and the sub-cycle AC Stark shift. Since experimental observations always result from propagation in a macroscopic gas, we also solve the Maxwell wave equation (MWE) for the time propagation of light fields through the atomic helium gas medium, in which the polarization and ionization source terms are obtained by solving the single-atom TDSE [13]. The absorption/emission probability after propagation of a dilute gas is almost identical to the single atom result in Fig. 1, exhibiting both the half-cycle modulations, the LISs, and the emission features discussed above. This indicates that our DDAA predictions can be observed using current attosecond technology, especially as it regards half-IR-cycle oscillations. We note that these interference features have been observed in a very recent experiment [25].

We have demonstrated that interference fringes in DDAA spectra result from the coherent addition of two quantum paths that lead to the same dipole excitation. They reveal the time delay between the initial excitation and a later, IR-field driven multiphoton transition. This was found to be true both for transitions between bound states as well as between excitation modes (the LISs) that are observable only when the pulses overlap. We expect that they will be a general feature in more complex systems, and could be observed between resonant states embedded in a continuum [2, 26]. Using this argument in reverse, the interference fringes visible in the DDAA spectrum could be used as a precise timing device, a probe of decoherence, or a phase meter when an intermediate resonance is involved.

Acknowledgements

This work was supported by the National Science Foundation under Grant No. PHY-0701372 and No. PHY-1019071. High-performance computational resources were provided by Louisiana State University (www.hpc.lsu.edu) and Louisiana Optical Network Initiative (www.loni.org).

[1] E. Goulielmakis, Z.-H. Loh, A. A. Wirth, R. Santra, N. Rohringer, V. Yakovlev, S. Zherebtsov, T. Pfeifer, A. Azzeer, M. Kling, *et al.*, Nature **466**. 739 (2010).
[2] H. Wang, M. Chini, S. Chen, C.-H. Zhang, Y. Cheng, F. He, Y. Cheng, Y. Wu, U. Thumm, and Z. Chang, Phys. Rev. Lett. **105**, 143002 (2010).
[3] J. Itatani, F. Quéré, G. L. Yudin, M. Y. Ivanov, F. Krausz, and P. B. Corkum, Phys. Rev. Lett. **88**, 173903 (Apr 2002).
[4] F. Krausz and M. Ivanov, Rev. Mod. Phys. **81**, 163 (Feb 2009).
[5] T. Remetter, P. Johnsson, J. Mauritsson, K. Varjú, F. L. Y. Ni, E. Gustafsson, M. Kling, J. Khan, R. López-Martens, K. J. Schafer, *et al.*, Nature Physics **2**, 323 (2006).
[6] J. Mauritsson, T. Remetter, M. Swoboda, K. Klünder, A. L'Huillier, K. J. Schafer, O. Ghafur, F. Kelkensberg, W. Siu, P. Johnsson, *et al.*, Phys. Rev. Lett. **105**, 053001 (Jul 2010).
[7] A. Wirth, M. T. Hassan, I. Grgura, J. Gagnon, A. Moulet, T. T. Luu, S. Pabst, R. Santra, Z. A. Alahmed, A. M. Azzeer, *et al.*, Science **334**, 195 (2011).
[8] M. Holler, F. Schapper, L. Gallmann, and U. Keller, Phys. Rev. Lett. **106** 123601, (2011).
[9] S. Chen, K. J. Schafer, and M. B. Gaarde, Optics Lett. **37**(12), 2211 (JUN 15 2012).
[10] M. Chini, B. Zhao, H. Wang, Y. Cheng, S. X. Hu, and Z. Chang, Phys. Rev. Lett. **109**, 073601 (Aug 2012).
[11] S. Chen, M. J. Bell, A. R. Beck, H. Mashiko, M. Wu, A. N. Pfeiffer, M. B. Gaarde, D. M. Neumark, S. R. Leone, and K. J. Schafer, Phys. Rev. A **86**, 063408 (Dec 2012).
[12] H. Paul, Optical and Quantum Electronics **28**, 1111 (1996).
[13] M. B. Gaarde, C. Buth, J. L. Tate, and K. J. Schafer, Phys. Rev. A **83**, 013419 (2011).
[14] J. C. Baggesen, E. Lindroth, and L. B. Madsen, Phys. Rev. A **85**, 013415 (Jan 2012).
[15] M. Lindberg and S. W. Koch, Phys. Rev. B **38**, 7607 (Oct 1988).
[16] C. H. B. Cruz and *et al.*, IEEE J. Quant. Electron. **24**, 261 (1988).
[17] B. H. Bransden and C. J. Joachain, *Physics of Atoms and Molecules* (Prentice Hall, 2003).
[18] M. Swoboda, T. Fordell, K. Klünder, J. M. Dahlström, M. Miranda, C. Buth, K. J. Schafer, J. Mauritsson, A. L'Huillier, and M. Gisselbrecht, Phys. Rev. Lett. **104**, 103003 (Mar 2010).
[19] T. Halfmann, L. P. Yatsenko, M. Shapiro, B. W. Shore, and K. Bergmann, Phys. Rev. A **58**, R46 (Jul 1998).
[20] M. S. Shahriar, P. Pradhan, and J. Morzinski, Phys. Rev. A **69**, 032308 (Mar 2004).
[21] T. Unold, K. Mueller, C. Lienau, T. Elsaesser, and A. D. Wieck, Phys. Rev. Lett. **92**, 157401 (Apr 2004).
[22] T. Guenther, C. Lienau, T. Elsaesser, M. Glanemann, V. M. Axt, T. Kuhn, S. Eshlaghi, and A. D. Wieck, Phys. Rev. Lett. **89**, 057401 (Jul 2002).
[23] J. J. Baumberg, B. Huttner, R. A. Taylor, and J. F. Ryan, Phys. Rev. B **48**, 4695 (Aug 1993).
[24] S. Pabst, A. Sytcheva, A. Moulet, A. Wirth, E. Goulielmakis, and R. Santra, Phys. Rev. A **86**, 063411 (Dec 2012).
[25] M. Chini, X. Wang, Y. Cheng, Y. Wu, D. Zhao, D. A. Telnov, S.-I. Chu, and Z. Chang, Scientific Reports **3** (2013).
[26] M. Tarana and C. H. Greene, Phys. Rev. A **85**, 013411

(Jan 2012).